npj | climate and atmospheric science

Article

Published in partnership with CECCR at King Abdulaziz University

https://doi.org/10.1038/s41612-026-01378-9

Analysis of the abundance and impacts of volatile organic compounds across Europe

Xiansheng Liu[1,2] ✉, Minghan Wang[1,2], Taicheng An[1,2], Xun Zhang[3] ✉, Tao Wang[4], Rosa Lara[5], Marta Monge[5], Marvin Dufresne[6], Ana Maria Yañez-Serrano[5,7,8], Roger Seco[5], Marie Gohy[9], Paul Petit[9], Audrey Chevalier[10], Marie-Pierre Vagnot[11], Yann Fortier[11], Alexia Baudic[12], Véronique Ghersi[12], Grégory Gille[13], Ludovic Lanzi[13], Valérie Gros[14], Jean-Eudes Petit[14], Leïla Simon[14,15], Heidi Hellén[16], Stefan Reimann[17], Zoé Le Bras[17], Michelle Jessy Müller[17], David Beddows[18], Siqi Hou[18], Zongbo Shi[18], Roy M. Harrison[18], William Bloss[18], James Dernie[19], Stéphane Sauvage[4], Alastair Lewis[20], Jim Hopkins[20], Xiaoli Duan[21], Philip K. Hopke[22,23], Andrés Alastuey[5], Xavier Querol[5] & Thérèse Salameh[6] ✉

Urban volatile organic compounds (VOCs) are key precursors of tropospheric ozone and secondary organic aerosols (SOA), yet their long-term dynamics and health implications remain unclear across Europe. Here, we synthesize two decades of VOC observations (2002–2023) from 21 urban monitoring sites in six countries to assess emission trends, oxidation potentials, and human exposure risks. Consistent declines in total hydrocarbons were observed at most sites, reflecting the effectiveness of emission control policies. Aromatic hydrocarbons such as toluene, xylene, and benzene were the dominant contributors to ozone and SOA formation. Physiologically based toxicokinetic (PBTK) modeling suggests that key VOCs preferentially accumulate in the kidney and liver. The integration of atmospheric monitoring with toxicokinetic modeling provides a multi-scale understanding of how urban VOCs influence both air quality and internal human exposure, offering new insight into effective pollution control strategies.

Volatile organic compounds (VOCs) are widely distributed in the atmosphere and play a pivotal role in air quality degradation, climate forcing, and human health impairment[1,2]. Since the pioneering work of Haagen-Smit (1952)[3], it has been recognized that VOCs, in the presence of nitrogen oxides ($NO_x = NO + NO_2$) and sunlight, drive the generation of tropospheric ozone (O_3) and secondary organic aerosols (SOA)—two key components of modern urban air pollution[4,5]. VOCs exhibit remarkable chemical and source diversity, with more than 300 species identified from both anthropogenic and biogenic origins[6]. Although biogenic emissions dominate the global VOC budget[7,8], urban atmospheres are largely controlled by anthropogenic VOCs (AVOCs) originating from traffic, industrial emissions, and solvent use, which remain the principal drivers of photochemical pollution[9].

Extensive studies in cities such as Los Angeles, Paris, and Beijing have demonstrated that VOC levels exhibit strong spatiotemporal variability, shaped by emission source profiles, meteorological conditions, and local control policies[10–12]. In recent years, non-combustion emissions from products, paints, and solvents have become increasingly important as vehicular exhaust contributions decline under stricter regulations[13]. Across Europe, official emission inventories indicate a marked decrease in non-methane VOC (NMVOC) emissions since the 1990s (Fig. S1), primarily due to technological upgrades and regulatory interventions. However, the ambient VOC composition has shifted, with solvent-related and oxygenated compounds becoming more dominant[14,15]. Despite these changes, most European VOC studies remain limited to individual countries or specific sources (e.g., road traffic), and few have systematically assessed VOC composition, reactivity, and their potential to form O_3 or SOA at a continental scale. The new European Air Quality Directive, which recommends monitoring 47 VOC species (Table S1), underscores the need for such harmonized and integrated assessments[16].

While ambient VOC monitoring provides crucial insights into external exposure, the internal toxicokinetics of VOCs within the human body remain poorly characterized[17]. Only limited studies have quantitatively linked ambient VOC concentrations to internal dose metrics[17,18], constraining accurate health risk assessments. Physiologically based toxicokinetic (PBTK) models, which simulate absorption, distribution,

A full list of affiliations appears at the end of the paper. ✉e-mail: xianshengliu@gdut.edu.cn; zhangxun@btbu.edu.cn; therese.salameh@imt-nord-europe.fr

metabolism, and excretion (ADME) processes of chemicals in human organs[19–22], offer a promising approach to bridge environmental exposure with internal biological dose. However, their integration into atmospheric VOC studies remains rare, leaving a major gap in connecting emission patterns to health-relevant internal exposure.

Against this background, this study aims to address three key questions[1]: *How have VOC concentrations and compositions evolved across European urban environments over the past two decades under emission control policies?*[2] *How do these spatiotemporal variations affect O_3 and SOA formation potentials?*[3] *What are the implications of observed VOC patterns for human internal exposure and health risk, as inferred from PBTK modeling?*

We hypothesize that the long-term evolution of VOCs in Europe reflects not only emission reductions but also a compositional transition that modifies photochemical reactivity and secondary pollutant formation, leading to heterogeneous health implications across urban regions. To test this hypothesis, we compiled and harmonized two decades of VOC observations (2002–2023) from 21 monitoring sites in six European countries (France, Belgium, Finland, the United Kingdom, Switzerland, and Spain) under the RI-URBANS project (https://riurbans.eu/). We quantified VOC spatiotemporal variability, estimated maximum O_3 and SOA formation potentials (MOFP and SOAP), and integrated a PBTK modeling framework for representative VOC species (benzene, toluene, ethylbenzene, and 1,2,4-trimethylbenzene). This integrative approach links emission trends, atmospheric chemistry, and toxicokinetics into a unified framework, offering a novel perspective on the exposure–dose–response continuum in the context of evolving European air quality policies.

Results

Spatiotemporal variability of VOCs in selected European urban

In Europe, there is currently no standardized reference instrumentation for measuring VOCs in ambient air. Although a working group under the European Committee for Standardization (CEN) is developing harmonized protocols, available datasets have been generated using diverse analytical methods, leading to inter-site inconsistencies. Direct comparison of VOC mixing ratios is further complicated by variations in the number and type of monitored compounds across sites. Among the 21 datasets compiled in this study, none covered all 47 VOCs recommended by the new European Air Quality Directive, highlighting the urgent need for method harmonization and standardized target compound lists. It should be noted that the spatial patterns and compositional characteristics discussed above are based on long-term average conditions, whereas temporal evolution and trend behavior are examined separately in the following section.

To ensure comparability among sites, 20 commonly measured VOCs were selected, defined as species that were consistently monitored across a minimum of 15 out of the 21 sites, ensuring sufficient spatial representativeness and comparability across the monitoring network (Table S1; Fig. S2). Across urban sites, total VOC mixing ratios (sum of 20 species) ranged from 2.1×10^3 to 1.9×10^4 ppt (Fig. S3). The highest concentrations were observed at industrial (LYO1_IND) and traffic (LND_TR) sites, while the lowest occurred at urban background locations (NAM_UB, MON_UB). This spatial pattern reflects dominant emission influences from industry and transportation in densely urbanized areas[23].

Additional spatial variability emerged when VOC concentrations were examined from a broader geographic perspective, beyond differences attributable to site type. To ensure comparability across countries and to address potential biases arising from mixed site classifications, country-level comparisons were restricted to UB sites only. This approach minimizes the influence of local emission hot spots (e.g., traffic or industrial sources) and allows for a more consistent assessment of regional-scale VOC characteristics. Specifically, 20 species were comparable for Belgium, France, and the United Kingdom; 12 species for Belgium, France, the United Kingdom, and Finland; 11 species for Belgium, France, the United Kingdom, Finland, and Switzerland; and benzene and toluene for all six countries (Belgium, France, the United Kingdom, Finland, Switzerland, and Spain) (Fig. S4). For the subset of 20 commonly measured species, UB sites in France exhibited the highest summed VOC mixing ratios, followed by the United Kingdom and Belgium. Similar patterns were observed for the 12-species subset, with France showing higher VOC levels than Finland and Belgium, although absolute values decreased with the reduced species coverage. For the 11-species subset, France and Switzerland showed higher summed VOC mixing ratios at urban background sites compared with Belgium and the United Kingdom. When the comparison was further restricted to benzene and toluene only, differences among countries became less pronounced, reflecting the more uniform regulation and long-term decline of these regulated compounds across Europe. A coastal–inland comparison based on the common 11-species subset further indicated higher summed VOC mixing ratios at coastal urban background sites than at inland sites (represented by Switzerland), suggesting that regional-scale factors such as maritime influence and emission source composition contribute to spatial variability beyond local urban conditions.

Beyond differences in total VOC levels, compositional analysis revealed that the ten most abundant species accounted for over 80% of total VOCs at most sites (except MAR_UB, where a broader measurement spectrum reduced this fraction to 70%). Alkanes (ethane, n-butane, propane) and aromatics (toluene, benzene, m,p-xylene) were the most prevalent compounds (Fig. 1). High fractions of C2–C4 alkanes at sites such as ANG_UB, HET_UB, and LYO_IND primarily reflect influences from natural gas-related emissions and fossil fuel combustion, rather than solvent evaporation, whereas aromatic dominance at HEL_UB and HEL_TR (>60%) reflects traffic-related and solvent-use emissions. These findings align with European emission inventories and previous urban studies in Asia reporting similar VOC signatures associated with fossil fuel use and solvent-related activities[24–26]. Specifically, BAQS_UB, BCN_UB, ZUR_UB, and PAR_SUB were the only sites measuring OVOCs. Alcohol compounds (methanol, ethanol) were predominantly found at these sites. This is likely due to increased reported emissions from the distilling industries, the use of alcohol as a solvent in personal care, car care and household products, gasoline, gasoline evaporation, biogenic sources, combined with their long atmospheric lifetime[14,27,28], highlighting the need to extend OVOC monitoring to additional sites.

When grouped by site type, industrial locations exhibited the highest total VOC mixing ratios, followed by traffic and urban background sites (Fig. S5). Alkanes and alkenes dominated at industrial sites, while aromatics were more abundant at traffic sites (excluding benzene). This suggests that industrial sources primarily contribute lighter alkanes, whereas vehicular and solvent-related activities remain key aromatic emitters across European cities.

Inter-annual trends of VOCs mixing ratios

Inter-annual trends were analyzed for datasets spanning more than five years, covering ten monitoring sites (CHM_UB, GRE_UB, HET_UB, LND_UB, MON_UB, STB_UB, LND_TR, LYO1,2_IND, and MSR_IND). Overall, total VOC (TVOC) mixing ratios exhibited distinct long-term patterns across Europe (Fig. 2). Among them, CHM_UB, HET_UB, MON_UB, and MSR_IND showed relatively stable TVOC levels with no significant overall change, although piecewise trend analysis revealed episodic increases and decreases within specific sub-periods (Table S2). LND_UB and LYO2_IND showed statistically significant downward trends with relatively smaller slope (−1.64[−2.33, −0.85] to −1.39[−2.35, −0.39] %/yr, $p < 0.05$), while GRE_UB, STB_UB, LND_TR, and LYO1_IND exhibited larger negative slopes indicating more pronounced declines (−2.65[−3.13, −2.05] to −3.21[−3.91, −2.41] %/yr, $p < 0.01$). These declines were mainly observed after 2010 and are temporally consistent with the period during which multiple emission control measures (e.g., European Directive on the reduction of national emissions (2016/2284/EC)) were implemented across Europe.

When examining individual VOC species, site-specific differences emerged (Figs. S6–S15). At stable sites (CHM_UB, HET_UB, MON_UB, MSR_IND), opposite-sign trends among VOCs (some

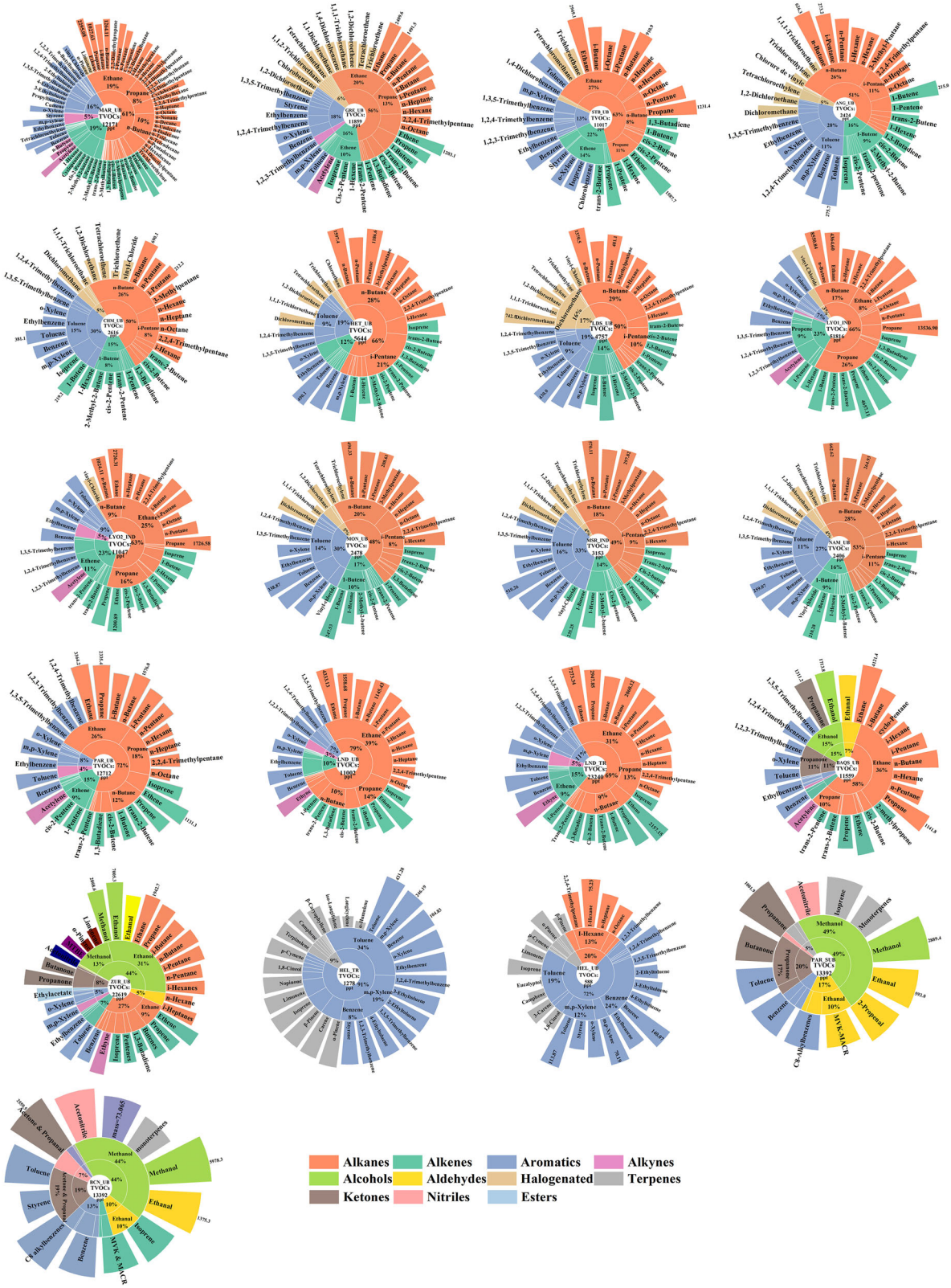

Fig. 1 | Composition of the VOC categories at 21 sites during 2002–2023. The contributions >8% were marked; the number in each left corner is the number of VOCs measured; note that sites are grouped by comparable measurement methods, and differences in VOC composition partly reflect variations in measurement coverage across sites.

increasing, some decreasing) offset each other, resulting in little overall change in TVOCs (Figs. S7, S9, S12–S14). In contrast, sites with declining TVOCs showed coherent decreases across most VOC classes, especially alkanes, alkenes, and aromatics, consistent with reductions in traffic and industrial emissions. Many traffic-related VOCs exhibited substantial reductions within a decade, aligning with previous reports for France[29] and the UK[14]. For instance, median toluene concentrations at traffic sites decreased from approximately 900–1200 ppt in the early

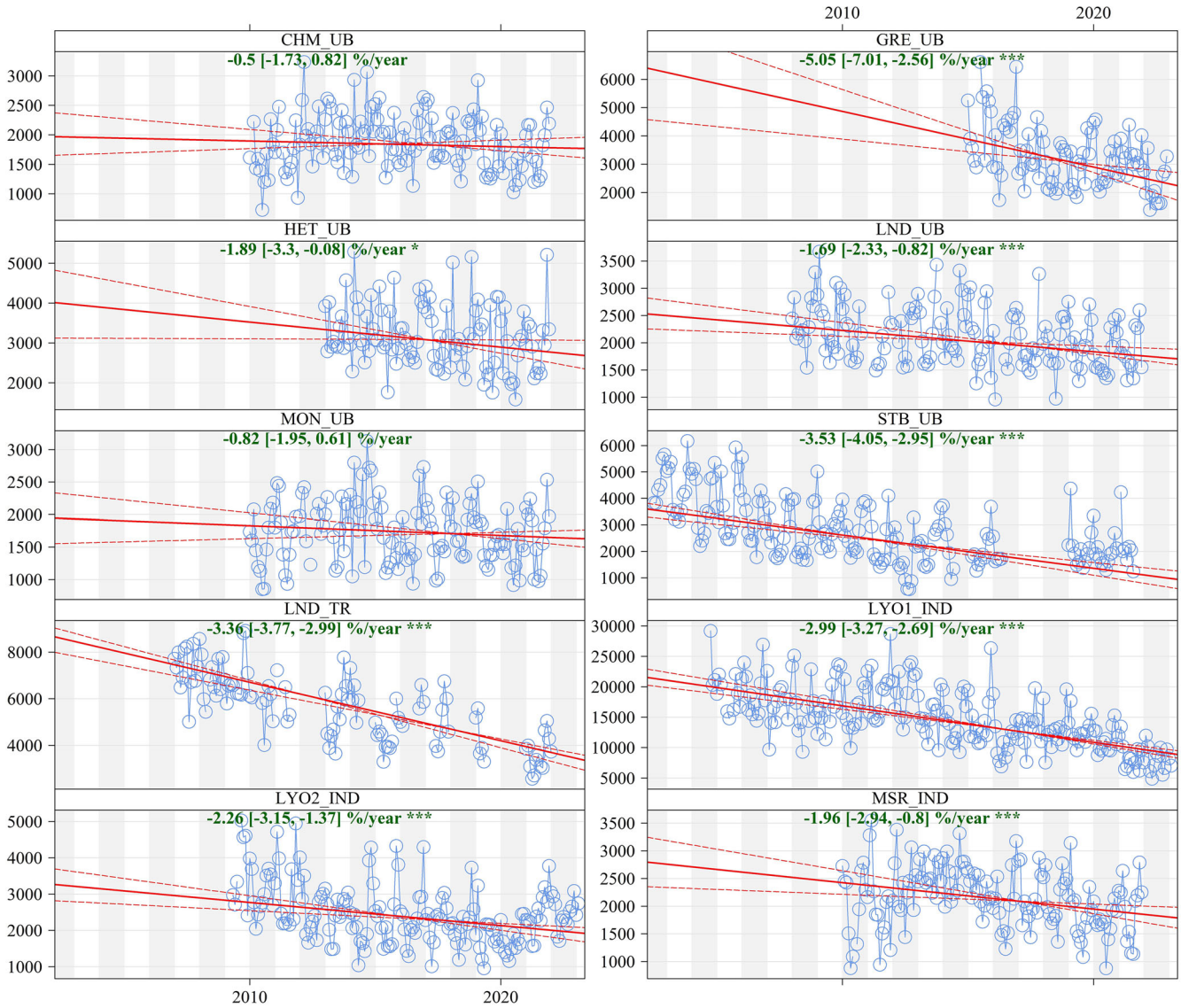

Fig. 2 | The trends in total VOC (TVOC) mixing ratios at the 10 sites with time series >5 years. Sen's slope of long-term period data is indicated in green, expressed as an average annual percent change. $p < 0.001$ = ***, $p < 0.01$ = **, $p < 0.05$ = *and $p < 0.1$ = +; (blank) non statistically significant.

2000s to below 300 ppt after 2015, corresponding to a reduction by a factor of about 3–4.

A meta-analysis integrating 18 representative VOCs confirmed a statistically significant overall decline (−2.38[−3.11, −1.66] %/yr) across all urban sites (Fig. 3). Alkanes and aromatics showed consistent downward trends of 2.56 to 3.65%/yr, while isoprene increased slightly at urban background sites but decreased at traffic and industrial sites (Table 1, Fig. S16). To further assess whether this divergence is driven primarily by seasonal meteorological variability, a deseasonalized trend analysis was conducted specifically for isoprene (Fig. S17). After removal of the climatological monthly cycle, the same contrasting trends persisted, with increases at urban background sites and decreases at traffic and industrial sites, indicating that the observed pattern is not driven by seasonality alone. At traffic sites, nearly all VOCs declined more sharply (2.23–7.40%/yr), indicating the effectiveness of vehicular emission reduction policies.

In summary, the long-term evolution of VOCs across European monitoring networks reveals a continent-wide decreasing trend since the early 2000s, albeit with local variability reflecting differences in emission sources, control measures, and climatic influences.

Ozone and SOA formation potentials of VOCs: spatial, seasonal, and long-term variability across European urban environments

The contributions of 20 VOCs with initial concentrations to the formation of maximum O_3 and SOA potentials were estimated using all datasets and presented in Fig. 4. Among them, toluene, m,p-xylene, 1-butene, n-butane, and isopentane accounted for 15% ± 9%, 13% ± 7%, 9% ± 8%, 9% ± 6%, and 7% ± 5% of MOFP, respectively. Together, they contributed over half of the total MOFP. For SOAP, aromatic hydrocarbons predominated (>85%), with toluene (55% ± 16%), benzene (20% ± 10%), m,p-xylene (7% ± 3%), and o-xylene (4% ± 2%) as the main contributors. These results highlight the key role of anthropogenic sources, particularly solvent and traffic-related emissions, in both ozone and SOA formation[26].

Spatial variability

The compositional patterns of MOFP and SOAP varied substantially among site types (industrial (IND), traffic (TR), urban background (UB); Fig. S18–S20). At UB sites, MOFP was mainly driven by toluene (16.2%), m,p-xylene (13.0%), and 1-butene (10.6%), whereas at TR sites, toluene (20.8%), m,p-xylene (19.3%), and n-butane (10.8%) dominated, reflecting the stronger influence of vehicular emissions. At IND sites, the top

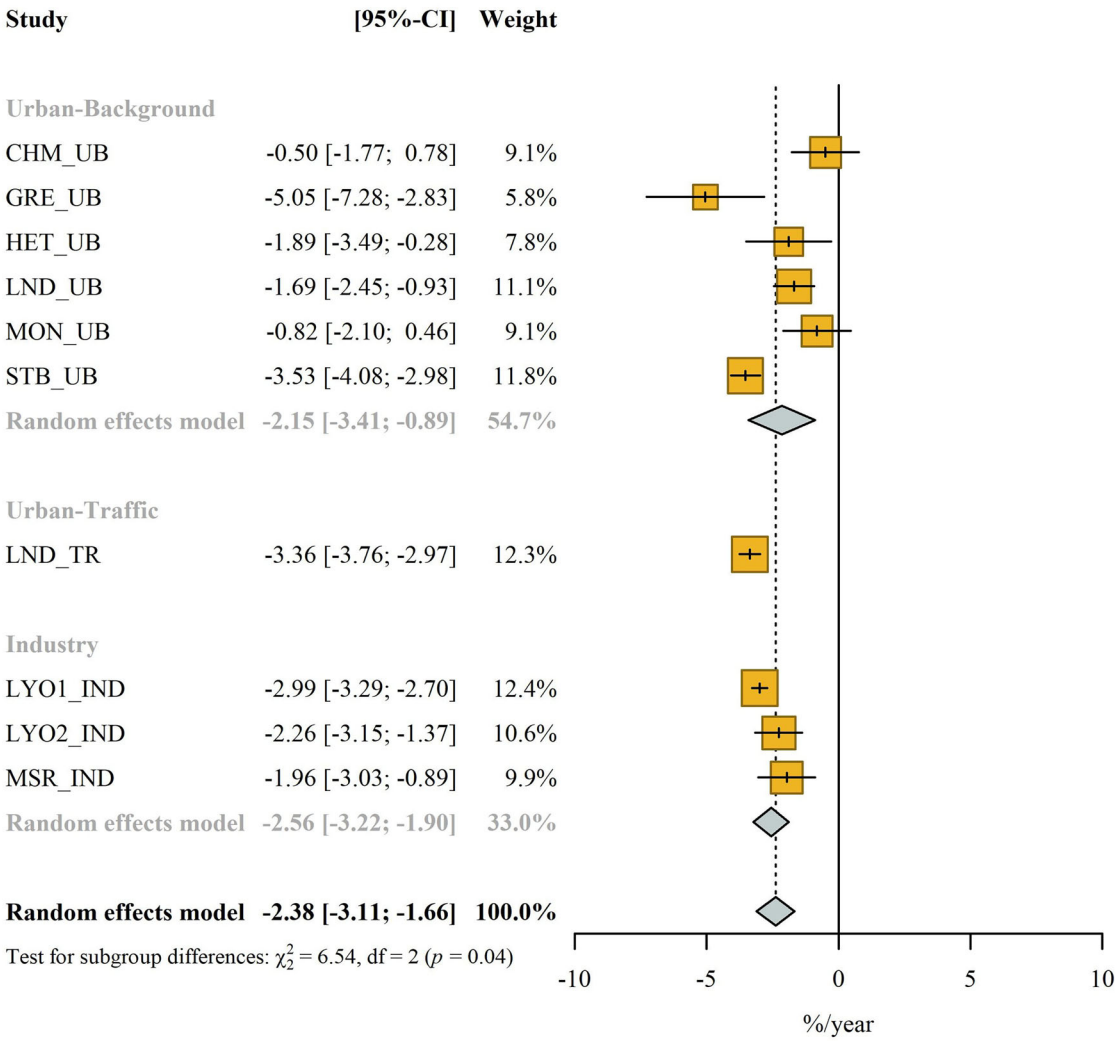

Fig. 3 | Meta-analysis results for the combined selected VOCs trends at 10 sites. The VOCs include n-butane, n-heptane, n-hexane, n-octane, n-pentane, cis-2-butene, trans-2-butene, 1-butene, isoprene, 1,3-butadiene, 1-pentene, benzene, toluene, m,p-xylene, o-xylene, 1,2,4-trimethylbenzene, 1,3,5-trimethylbenzene, ethylbenzene. Values are given and represented for slope [95% CI] in %/yr.

contributors were m,p-xylene (11.5%), trans-2-butene (11.1%), and toluene (10.9%), indicative of mixed industrial and solvent-related sources. For SOAP, aromatic hydrocarbons consistently prevailed across all site types, but their relative importance differed. Toluene and benzene together accounted for ~80% at UB and TR sites, while 1,3-butadiene replaced benzene as a key contributor (11.7%) at IND sites, pointing to petrochemical and rubber-related processes. These spatial contrasts are consistent with previous VOC source apportionment results[30], suggesting that traffic and industrial/solvent activities are the dominant drivers of O_3 and SOA formation in European urban areas. The dominance of aromatics in both MOFP and SOAP further suggests that ozone and SOA share common anthropogenic precursors, emphasizing the need for integrated emission reduction strategies targeting aromatic VOCs.

Seasonal variability

Seasonal analysis revealed that toluene and m,p-xylene remained major MOFP contributors year-round (Fig. S21–S24). Isoprene exhibited a stronger influence during summer, linked to higher temperature and solar radiation[31,32]. Stavrakou et al. (2014) investigated the factors influencing isoprene emissions in Asia between 1979 and 2012[33]. They discovered that the increase in temperature and sunlight resulted in an annual increase of 0.52% in emissions from China. This emphasizes the significant contribution of BVOCs to O_3 formation, stressing the importance of considering their impact alongside anthropogenic VOC emissions in comprehending and addressing the dynamics of O_3 production[34] and the importance of monitoring BVOCs in urban areas. In contrast, SOAP composition was less seasonally variable: BTEX species (benzene, toluene, ethylbenzene, xylenes) consistently dominated, highlighting the persistent contribution of solvent and fuel-related emissions to SOA formation across all seasons[35].

Long-term variability

To examine long-term evolution patterns, ten sites with continuous VOC observations exceeding five years were analyzed using heatmaps of MOFP and SOAP contributions (Fig. 5). The composition of dominant MOFP precursors was generally stable, though occasional ranking shifts occurred (e.g., alternation between toluene and 1-butene at CHM_UB, consistent dominance of m,p-xylene and toluene at GRE_UB). In contrast, gradual compositional transitions emerged at some sites (e.g., increasing influence of i-pentane and trans-2-butene at HET_UB and STB_UB), reflecting evolving traffic and industrial structures. For SOAP, toluene and benzene remained the leading contributors at most sites, except at STB_UB, where 1,3-butadiene rose sharply after 2018, surpassing benzene (>25%) and indicating a shift toward petrochemical emissions. Overall, aromatic VOCs have remained the principal SOA precursors over the past two decades, but site-specific transitions—particularly the growing importance of unsaturated

Table 1 | The meta-analysis results for selected VOCs trends at 10 monitoring sites

VOCs	UB	TR	IND	Total	*p*
n-butane	0.04 [−1.66, 1.74]	−2.78 [−3.49, −2.07]	−1.71 [−3.77, 0.36]	−0.89 [−2.16, 0.39]	<0.01
n-pentane	−3.44 [−7.32, 0.45]	−4.09 [−4.42, −3.76]	−2.29 [−4.62, 0.05]	−3.12 [−5.41, −0.84]	0.31
n-hexane	−3.63 [−4.98, −2.28]	−4.18 [−4.65, −3.70]	−1.93 [−3.48, −0.37]	−3.16 [−4.18, −2.14]	0.02
n-heptane	−2.56 [−4.85, −0.28]	−2.23 [−2.88, −1.57]	−2.52 [−5.36, 0.33]	−2.59 [−4.04, −1.14]	0.95
n-octane	−3.65 [−5.62, −1.69]	−0.30 [−1.24, 0.63]	−2.66 [−4.60, −0.72]	−2.99 [−4.39, −1.59]	<0.01
1,3-butadiene	−1.71 [−2.69, −0.73]	−7.40 [−7.88, −6.92]	−4.09 [−6.64, −1.54]	−2.91 [−4.51, −1.32]	<0.01
1-butene	−0.66 [−2.30, 0.98]	−3.35 [−3.88, −2.82]	−2.22 [−3.06, −1.37]	−1.44 [−2.57, −0.31]	<0.01
1-pentene	−0.28 [−2.54, 1.97]	−5.15 [−5.40, −4.90]	−4.59 [−4.81, −4.37]	−2.01 [−3.88, −0.15]	<0.01
trans-2-butene	−2.36 [−5.05, −0.33]	−6.00 [−6.95, −5.04]	−3.18 [−3.74, −2.61]	−2.84 [−3.99, −1.69]	<0.01
cis-2-butene	−2.22 [−2.83, −1.61]	−5.93 [−6.57, −5.30]	−3.27 [−3.69, −2.85]	−3.03 [−3.92, −2.15]	<0.01
benzene	−2.23 [−3.87, −0.58]	−3.22 [−3.64, −2.80]	−2.77 [−4.56, −0.99]	−2.59 [−3.59, −1.60]	0.48
toluene	−3.42 [−5.07, −1.76]	−4.81 [−5.12, −4.19]	−4.05 [−5.42, −2.68]	−3.82 [−4.82, −2.81]	0.17
m,p-xylene	−2.72 [−4.41, −1.04]	−4.85 [−5.33, −4.37]	−2.95 [−4.07, −1.83]	−3.03 [−4.11, −1.96]	<0.01
o-xylene	−2.64 [−5.78, 0.50]	−4.06 [−4.46, −3.67]	−1.66 [−3.42, 0.11]	−2.47 [−4.37, −0.58]	0.02
ethylbenzene	−2.77 [−4.79, −0.75]	−4.09 [−4.52, −3.67]	−2.66 [−3.27, −2.05]	−2.84 [−4.03, −1.65]	<0.01
1,2,4-trimethylbenzene	−2.36 [−5.05, 0.33]	−4.94 [−5.43, −4.45]	−2.61 [−4.30, −0.92]	−2.77 [−4.40, −1.14]	<0.01
1,3,5-trimethylbenzene	−2.65 [−4.72, −0.57]	−4.40 [−4.77, −4.03]	2.42 [−7.67, 12.52]*	−1.64 [−4.34, 1.06]	0.11
isoprene	2.77 [0.26, 5.29]	−5.66 [−8.93, −2.39]	−2.14 [−3.97, −0.30]	0.19 [−2.20, 2.58]	<0.01

*Note: For some species–site combinations (e.g., 1,3,5-trimethylbenzene at industrial sites), wide confidence intervals reflect limited data availability and/or high temporal variability, and results should therefore be interpreted with caution.

UB urban background, *TR* traffic, *IND* industry. Total: all sites considered.

hydrocarbons—highlight the dynamic nature of emission sources and the necessity of continuous VOC speciation monitoring.

Health risk of VOCs based on internal exposure

The PBTK model was applied to simulate the internal distribution of benzene, toluene, ethylbenzene, and 1,2,4-trimethylbenzene across major human organs/tissues and compartments, including blood, plasma, liver, kidney, lung, and gut, while other minor organs/tissues (e.g., muscle, adipose, brain, and skin) were collectively represented as a composite "rest" compartment[36] (Figs. S25 and S26). For each compound, the model outputs represent the maximum internal concentrations achieved within a daily exposure period under the corresponding ambient VOC levels. Across all compounds, simulated internal concentrations ranged from 10^{-4}–10^{-3} μmol/L, with the highest levels found in the kidney, followed by the liver, and the lowest in venous blood, showing significant organ-specific variability ($p < 0.01$). Average kidney concentrations were 6.2–10.9 times greater than those in venous blood, indicating strong organ-specific accumulation. This pattern aligns with physiological processes, as the liver and kidneys are the primary metabolic and excretory organs, respectively. Among the four VOCs, toluene showed the highest internal concentrations across all organs, consistent with its higher ambient levels and stronger bioaccumulation potential. These findings suggest that toluene is a pollutant of particular concern due to its higher internal burdens in metabolically active organs, warranting further investigation of its potential health relevance[37].

Spatial variations in internal VOC burdens mirrored those of external exposure (Fig. 6). Significant differences ($p < 0.01$, Kruskal–Wallis test) were found both among compartments at the same site and among sites for the same compartment. For benzene, internal concentrations followed the order IND > TR > UB > SUB, while for toluene, the pattern was TR > IND > UB > SUB. Ethylbenzene and 1,2,4-trimethylbenzene also showed elevated internal burdens at traffic and industrial sites (TR ≥ IND > UB), reinforcing that emissions from transportation and industrial activities are dominant contributors to human VOC exposure. Although modeled compartment concentrations were below current safety thresholds, evidence increasingly indicates that chronic, low-dose exposure to chemical mixtures may still cause adverse health outcomes. Caporale et al. (2022) estimated that exposure to endocrine-disrupting chemical (EDC) mixtures, even within regulatory limits, can lead to measurable health effects[38], while Liew and Guo (2022) emphasized that single-compound assessments may underestimate risks arising from chemical interactions[39]. Overall, these results indicate that internal VOC exposure is governed by both ambient concentrations and compound-specific toxicokinetics.

Discussion

The spatial pattern of VOC concentrations and ozone formation potentials reflects the dominant influence of emission sources across regions. Industrialized areas exhibit elevated levels of aromatics and alkanes, consistent with solvent use and petrochemical activities, while traffic-dominated environments are characterized by high proportions of alkenes and BTEX compounds. These findings align with a previous study in Spain[26], which similarly highlighted the dominance of aromatic hydrocarbons in SOA formation. This underscores the role of transportation and industrial activities as primary sources of VOCs contributing to secondary aerosol production across Europe[35]. Meteorological conditions further modulate VOC variability, as higher temperatures and stagnant air masses enhance photochemical activity and secondary formation potential[31,32], particularly during summer episodes. Regional differences in control strategies also play a role: countries with stringent industrial emission regulations show relatively lower aromatic concentrations, whereas weaker traffic management policies contribute to persistently high levels in urban cores. The co-dominance of aromatics and alkenes in many sites emphasizes the need for integrated emission reduction strategies that simultaneously target industrial solvent use and vehicular exhaust to effectively mitigate ozone formation across Europe.

Beyond these general source-related patterns, our results further showed pronounced spatial differences in VOC abundance and formation potentials across European regions. When comparisons were restricted to harmonized VOC subsets measured at urban background sites, VOC concentrations in France generally exhibited higher total VOC levels and ozone formation potentials than those in Belgium and Finland, while values in the United Kingdom were comparable, depending on the species subset

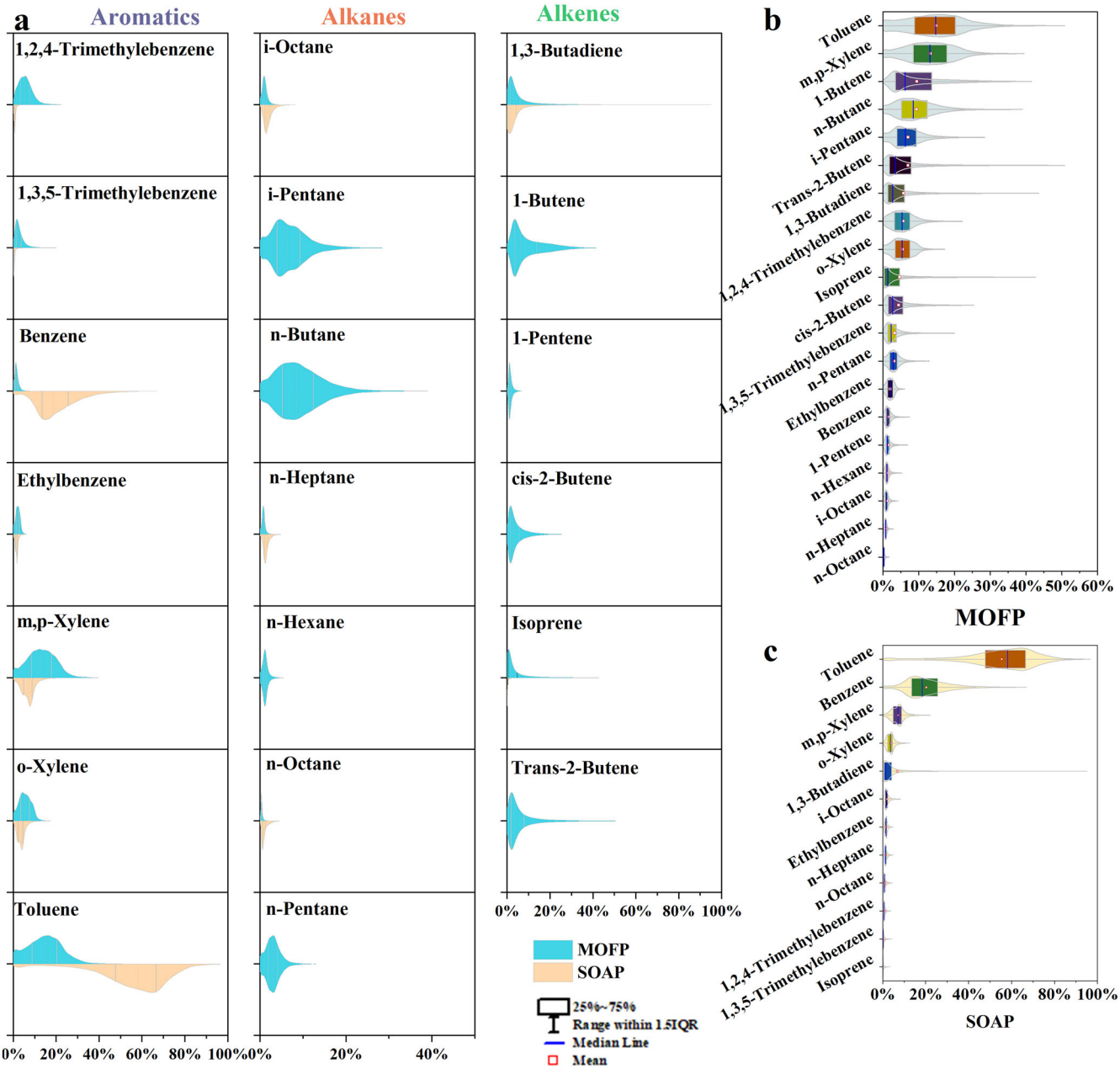

Fig. 4 | Comparison of VOC contributions to ozone and secondary organic aerosol formation potential across datasets. Panel (**a**) compares the contributions of 20 VOCs to maximum O_3 formation potential (MOFP) and secondary organic aerosol potential (SOAP) across all datasets. Violin plots illustrate the distribution of fractional contributions, with the width of each violin representing the probability density of the data along the x-axis. Panels (**b**) and (**c**) show the ranking orders of the 20 VOCs according to their contributions to MOFP and SOAP, respectively.

considered. These country-level differences are unlikely to be solely attributable to site classification or measurement coverage. Instead, they likely reflect a combination of region-specific emission intensity, differences in VOC speciation, and the long-term effectiveness of emission control policies, rather than local source influences alone.

A clear coastal-inland contrast emerges, with higher VOC concentrations observed in coastal countries compared with inland Switzerland under identical species coverage. Long-term observations at suburban and urban sites in Switzerland showed a sustained decline of BTEX concentrations by up to ~80–90% over the past three decades, largely attributed to stringent and long-standing VOC control measures targeting traffic fuel composition and solvent use, resulting in a markedly reduced contribution of aromatic VOCs to the urban VOC mixture[40]. An additional contributing factor may be the limited regulation of VOC emissions from maritime transport, which disproportionately affects coastal regions. Recent land-based, high time-resolution observations in a Sulfur Emission Control Area (SECA) in northern France demonstrated that ship emissions were associated with substantial VOC emissions, including oxygenated compounds and aromatic VOCs, even under strict SO_2 and NO_x control regimes[41]. This regulatory gap in shipping-related VOC emissions is likely to enhance VOC abundance and photochemical reactivity in coastal environments, contributing to the observed coastal–inland differences in VOC impacts across Europe. Taken together, to place these formation potential patterns in a broader atmospheric context, we qualitatively compared the spatial distribution of MOFP and SOAP with reported regional patterns of surface ozone and $PM_{2.5}$ across Europe, as documented by the European Environment Agency (EEA). Regions characterized by elevated MOFP and SOAP values are broadly consistent with areas where higher secondary

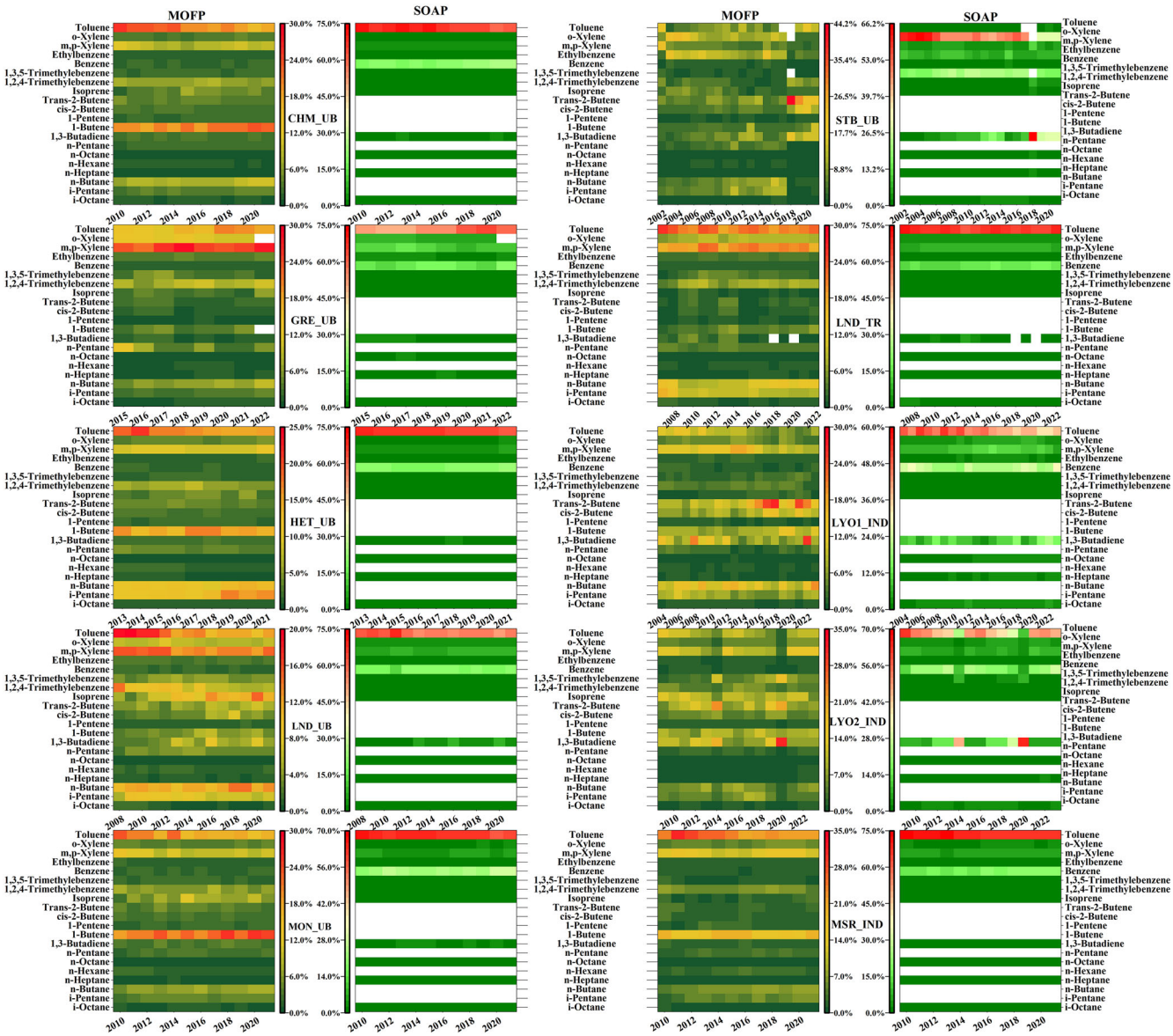

Fig. 5 | Interannual variations in VOC contributions to ozone and secondary organic aerosol formation potential. Heatmaps show the interannual variations in the contributions of 20 VOC species to maximum O_3 formation potential (MOFP) and secondary organic aerosol potential (SOAP) at 10 monitoring sites, visualized as heatmaps. White blocks represent missing values. Due to differences in monitoring periods across sites, temporal variations are interpreted on a within-site basis rather than through direct inter-site comparisons.

pollution burdens are commonly reported at regional and long-term scales, while regions with lower formation potentials tend to exhibit comparatively lower reported secondary pollutant concentrations.

The long-term evolution of VOC concentrations observed in this study can be further linked to the progressive implementation of emission control policies across Europe. A critical transition period occurred between 2000 and 2005, coinciding with the implementation of the Euro III (2000) and Euro IV (2005) standards for heavy-duty vehicles, as well as the Euro 3 (2000) and Euro 4 (2005) standards for light-duty vehicles. Both regulatory streams tightened limits on hydrocarbon emissions (e.g., NMHC/THC, depending on vehicle/fuel category), thereby contributing to reductions in traffic-related VOCs. For gasoline vehicles, three-way catalytic converters were introduced earlier (from Euro 1 onward) and are not applicable to diesel vehicles; in contrast, many light-duty diesel vehicles were equipped with oxidation catalysts, with broader adoption driven in part by Euro 3 requirements[42,43]. European-scale analyses have shown that during this period, road transport emissions became progressively decoupled from fuel consumption, with sustained reductions in NMVOC and NOx emissions despite stable or increasing traffic volumes[42,44]. More recently, the introduction of the Worldwide Harmonized Light Vehicles Test Procedure (WLTP) and real driving emissions (RDE) requirements after 2017 further strengthened vehicular emission regulation by narrowing the gap between laboratory testing and real-world driving conditions[45]. In parallel, changes in fuel formulation, including the increasing use of bioethanol-blended gasoline across Europe, have contributed to reductions in aromatic content and shifts in VOC speciation[46]. Together, these measures provide a coherent regulatory and technological context for the pronounced long-term decline of traffic-related aromatic VOCs and their dominant contributions to MOFP and SOAP observed at many urban sites in this study.

Beyond the transport sector, additional reductions in anthropogenic VOC emissions across Europe have been supported through national implementation frameworks established under the Directive (EU) 2016/2284[47]. Under this framework, EU Member States are required to prepare and implement National Air Pollution Control Programs (NAPCPs), which define policy priorities and measures to reduce emissions of regulated pollutants, including NMVOCs. In addition, National Energy and Climate

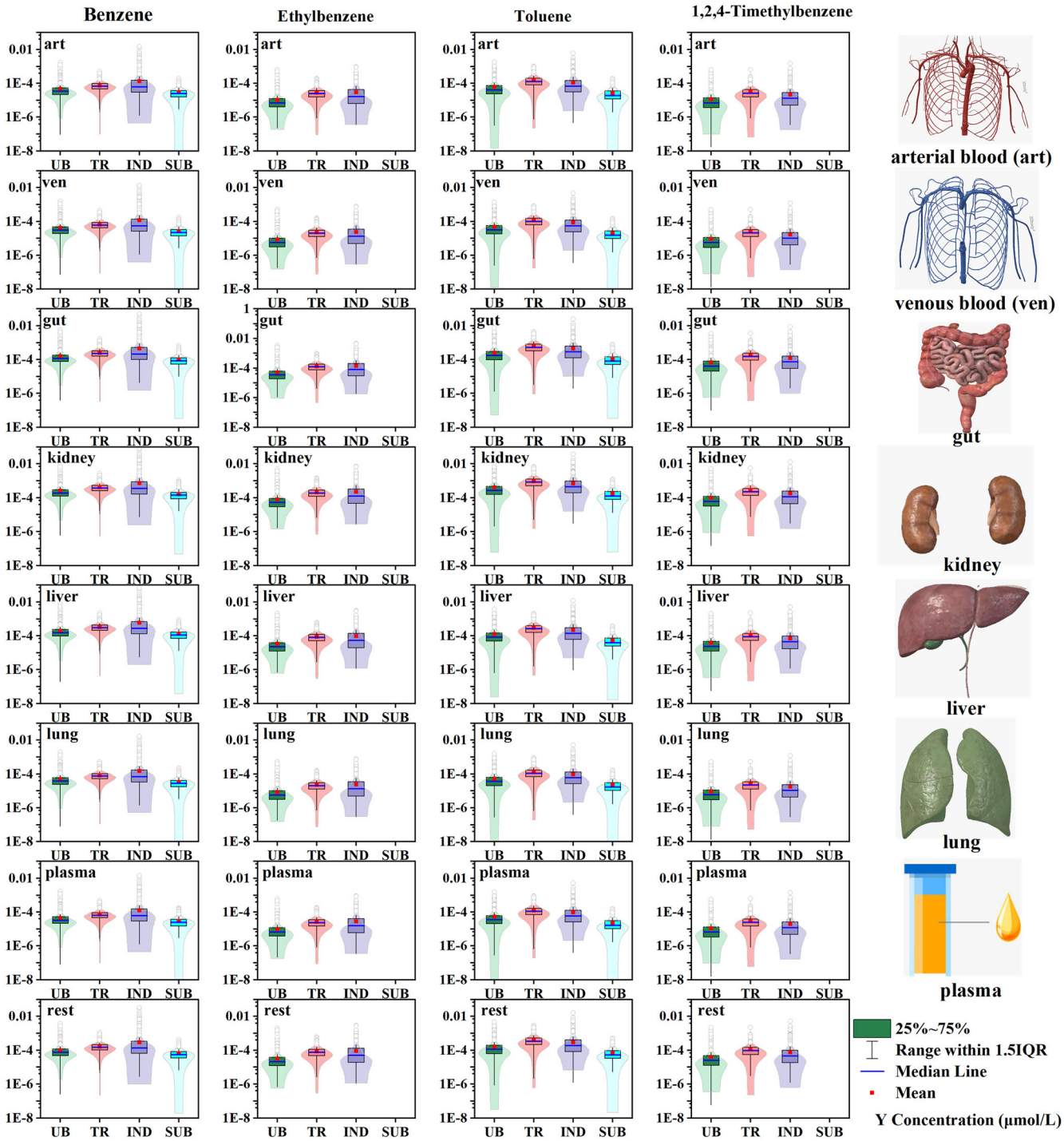

Fig. 6 | Simulated internal exposure levels of representative volatile organic compounds across human organs and tissues. Panels show the simulated internal exposure levels of four representative VOCs (benzene, toluene, ethylbenzene, and 1,2,4-trimethylbenzene) across major human organs/tissues and compartments, including arterial blood (Art), venous blood (Ven), gut, kidney, liver, lung, plasma, and the rest of the body (Rest), at different types of monitoring sites (UB urban background, TR traffic, IND industrial, SUB suburban). The "Rest" compartment represents all organs/tissues not explicitly modeled, such as adipose, brain, skin, heart, bone marrow, and muscle. Organ illustrations were created based on a 3D human body model provided by 3Dbody (© 2012–2025 3Dbody). Reproduced/adapted with permission.

Plans (NECPs), developed to meet EU-wide 2030 energy and climate targets, include complementary measures, such as energy system transformation, fuel switching, and industrial modernization, that further contribute to NMVOC emission reductions[48].

From a human health perspective, PBTK modeling revealed that aromatic hydrocarbons such as toluene and benzene exhibit the highest internal accumulation, particularly in the kidney and liver. These finding highlights that even when ambient VOC concentrations comply with existing air quality standards, internal body burdens can remain non-negligible due to bioaccumulation and chronic exposure. Among these compounds, toluene represents a major pollutant of concern because of its widespread urban presence and high tissue affinity[49]. Chronic low-dose exposure has been associated with neurotoxic and hepatotoxic effects, suggesting potential underestimation of health risks in current outdoor exposure assessments[50,51]. These results underscore the need to integrate internal exposure modeling into routine air-quality evaluations, enabling a

more realistic estimation of population-level risks. From a regulatory perspective, most European directives currently focus on ambient concentration thresholds rather than cumulative internal doses or mixture effects. Incorporating internal dose metrics and multi-pollutant risk frameworks could provide a more health-protective approach, aligning with the World Health Organization's call for cumulative exposure assessment. Overall, the combination of long-term VOC trends with toxicokinetic modeling provides a bridge between emission control and human health protection, supporting evidence-based policy refinement across European urban environments. Future health risk assessments should therefore incorporate multi-pollutant interactions and dynamic internal exposure modeling to more accurately characterize cumulative health risks in urban environments.

This study provides one of the most comprehensive assessments of urban VOC variability across Europe, integrating two decades of data from 21 monitoring sites in six countries. By harmonizing 116 VOC species, it offers new insights into temporal trends, spatial heterogeneity, and the evolving roles of key precursors such as toluene, benzene, and xylenes in ozone and SOA formation. The use of a PBTK model further bridges atmospheric concentrations and internal exposure, identifying the liver and kidney as major accumulation organs and establishing a mechanistic link between environmental levels and health risks.

Nevertheless, several limitations should be acknowledged. The meta-analysis focuses on 18 hydrocarbons consistently measured across all sites, which ensures comparability but excludes oxygenated and biogenic VOCs that are crucial for secondary formation processes. Although photochemical age-based reconstruction was applied to reduce degradation bias, expanding the monitoring of oxygenated and biogenic species remains essential. In addition, differences in instrumentation, detection limits, and sampling intervals across networks may introduce uncertainties. However, the trend for each site itself should be consistent. In the future, rigorous harmonization and quality control procedures should be adopted, and a standardized VOC measurement framework should be developed across Europe in alignment with the forthcoming Air Quality Directive.

Third, although the PBTK modeling framework provides a mechanistic representation of toxicokinetic processes, it relies on simplifying assumptions. Exposure inputs were specified at a daily time scale, and model outputs were summarized as daily peak internal concentrations under outdoor inhalation scenarios. Consequently, the simulations capture integrated organ-level burdens driven by ambient conditions but cannot fully resolve short-term variability in exposure. In addition, exposure concentrations were derived from outdoor measurements assuming an 8 h daily inhalation period, whereas real-world personal exposure is influenced by indoor environments and individual activity patterns. Therefore, the modeled internal doses should be interpreted as outdoor exposure-driven estimates rather than total personal exposure. Future studies incorporating higher temporal resolution exposure data, indoor–outdoor integrated assessments, population-specific physiological parameters, and multi-chemical interaction modeling would further enhance the realism and applicability of toxicokinetic-based exposure assessment.

Methods

Cities and sites providing VOCs data

This study compiled data from various locations across Europe, including Belgium (7 sites), Finland (2 sites), France (7 sites), Switzerland (1 site), Spain (1 site), and the UK (3 sites). The dataset comprised 3 IND, 2TR, 15 UB sites, and 1 suburban background (SUB) site (Fig. S27). These data were provided by regional air quality monitoring networks and research supersites within the RI-URBANS project. The site selection process was guided by several key criteria to ensure representativeness and data quality. First, sites were chosen to cover a broad range of urban areas across six European countries, capturing diverse climatic zones and population densities. This approach allowed the study to investigate VOC concentrations and variability under different environmental and urban conditions. Second, the selection included a variety of emission source types, encompassing industrial, traffic, urban background, and suburban settings, ensuring that key emission sources and ambient air conditions were comprehensively represented. Third, only sites with sufficient VOC monitoring data were included to enable robust trend analysis. Finally, many of the selected sites were part of established monitoring networks or supersites, ensuring high-quality data collection protocols and alignment with international monitoring standards. The abbreviated names of these sites are as follows:

- IND: Lyon Feyzin (LYO1), Lyon Vernaison (LYO2), and Mouscron (MSR).
- TR: Helsinki (HEL) and London (LND).
- UB: Angleur (ANG), Birmingham (BAQS), Barcelona (BCN), Charleroi (CHM), Grenoble (GRE), HEL, Herstal (HET), Lodelinsart (LDS), LND, Marseille (MAR), Mons (MON), Namur (NAM), Paris (PAR), Strasbourg (STB), and Zurich (ZUR).
- SUB: PAR

Measurements

Measurements of VOCs were performed at various stations using diverse analytic protocols/ methods, as outlined in Table S3. The instrumentation and models employed encompass thermal desorption gas chromatography with flame ionization detectors (TD-GC-FID/2FID), thermal desorption gas chromatography-mass spectrometry (TD-GC-MS), proton transfer reaction-time of flight-mass spectrometry (PTR-TOF-MS), PTR-Quad-MS, and passive samplers. Specifically, among the monitoring stations, at 10 out of 21 stations (C_2–C_9), species were measured. At 7 out of 21 stations (C_4–C_9), chloroethane and chloroethene species were identified. Other stations measured distinct combinations of VOCs, including C_6–C_9 aromatics and C_5–C_{15} BVOCs (HEL_TR), C_5–C_{10} and C_1–C_4 oxygenated VOCs (OVOC) and acetonitrile (BCN_UB), C_7–C_{10} and C_5–C_{10} BVOC (HEL_UB), and OVOC, along with some C_5–C_9 (PAR_SUB). These investigations highlight a varied approach to VOCs monitoring, encompassing a diverse array of compounds and utilizing different instruments and models across various monitoring stations. Specifically, all monitoring stations monitored benzene since it is regulated, and its homologs.

Data treatment

Data quality was assessed and evaluated by two ACTRIS CiGas units (IMT Nord Europe, France and EMPA, Switzerland) following ACTRIS and RI-URBANS recommendations and guidelines[52,53]. These guidelines provided a harmonized framework for VOC measurements across Europe, including standardized procedures for sampling, calibration, data validation, and intercomparison exercises. Several sites reported full compliance with ACTRIS protocols, particularly for GC-based measurements. Quality control procedures applied in this study included consistency checks for temporal continuity, screening for extreme or non-physical values, and verification of measurement completeness, in line with ACTRIS and WMO/GAW recommendations. Outliers identified during quality screening were removed prior to analysis to minimize the influence of episodic or non-representative events. For cross-site analyses, VOC datasets were harmonized by restricting comparisons to a common subset of species with sufficient data coverage, acknowledging that not all monitoring stations measured the full list of regulated VOCs. To reduce potential method-dependent biases arising from differences in instrumentation, analytical techniques, and monitoring periods, subsequent analyses focused on relative temporal trends and compositional patterns rather than absolute concentration levels.

All VOC data were standardized to mixing ratios in parts per trillion by volume (ppt), as recommended by the International Union of Pure and Applied Chemistry and a recent study[24]. This approach reduces variability caused by instrument differences and emphasizes the contribution of low molecular weight species relevant to O_3 and SOA formation[54]. Accordingly, VOC levels are presented as average mixing ratios ± standard deviation in ppt. These statistical analyses were conducted using SPSS software (IBM SPSS Statistics 25, Chicago, IL, USA). Differences in the number of VOC

species measured and instrumental sensitivity across sites were acknowledged and considered when interpreting site-to-site contrasts, as such differences may partly reflect measurement coverage rather than purely atmospheric variability.

Given the differences in monitoring methods across sites, our dataset inherently exhibits certain limitations, particularly due to the coexistence of online and offline sampling approaches. Online monitoring using PTR-TOF-MS and TD-GC-FID/2FID provides high temporal resolution (hourly data), whereas offline sampling with passive samplers typically offers lower resolution (weekly data). As a result, discrepancies in data resolution exist across sites. To address this issue, we standardized the data resolution to a weekly basis, ensuring a uniform framework for comparing mean VOC concentrations. This normalization helps minimize inconsistencies arising from varying temporal resolutions and enables more robust cross-site comparisons. Statistically significant differences in VOC concentrations at different monitoring sites were studied using the Kruskal-Wallis ANOVA on ranks[55] which was performed using the SPSS Software (IBM SPSS Statistics 25, Chicago, IL, USA). Subsequently, the study employed the Mann-Kendall (MK) test[56,57] along with the Theil-Sen estimator[58] to elucidate the interannual trend in VOCs mixing ratios and identified breakpoints and segmented slopes through piecewise linear regression using the R segmented package[59]. The individual slopes estimated as a percentage change per year with 95% CI (confidence interval), extracted from the Mann–Kendall test, were summarized by meta-analysis using the "meta" R package version 6.5-0[60]. The analysis is based on a random-effects model due to the heterogeneity of the data among the included sites, which involves variability in the effect sizes. The mean effect was calculated for each class of site individually (Industry, urban-traffic, urban-background, suburban-background and regional-background) as well as globally to provide a comprehensive overview of the results. Sen's method was utilized to estimate the slope of the trend. The significance level and Sen's slope value were assessed to clarify the interannual trend in VOCs levels, whether it was increasing or decreasing. Notably, since the MK and Sen's method are suited for datasets spanning more than 5 years, this study specifically focused on VOCs data from ten selected sites (CHM_UB, GRE_UB, HET_UB, LND_UB, MON_UB, STB_UB, LND_TR, LYO1_IND, LYO2_IND, and MSR_IND) for analysis. Meanwhile, for the meta-analysis of combined VOCs across 10 urban monitoring sites, we specifically selected VOC species (18 in total) that were consistently measured at all sites. This approach ensures that the observed trends reflect genuine atmospheric variations rather than discrepancies in data availability.

Estimating initial concentrations based on photochemical age

VOCs undergo varying degrees of photochemical loss during their transport from the source to the receptor[25]. More reactive species experience greater photochemical losses, making the directly measured VOC concentrations unsuitable for immediate source apportionment. The concentration ratio method is frequently used to calculate the photochemical age or ·OH exposure ([·OH]Δt) of an air mass and has been successfully applied in previous study[25]. Commonly used hydrocarbon compounds for this purpose include 1,3,5-trimethylbenzene/ethylbenzene (TMB/E), ethylbenzene/m,p-xylene (E/X), o-xylene/benzene (X/B), toluene/benzene (T/B), and propene/ethene (propene/ethene). In this study, the species used were ethylbenzene and m,p-xylene (correlation coefficient, $r > 0.8$). Assuming a constant volume fraction of ·OH and negligible background reactivity of VOCs[61], the initial photochemical concentrations of source emissions can be estimated using Eqs. (1) and (2) All OH reaction rate constants (ki[OH]) for VOC species were obtained from literature[25].

$$\left[VOC_i\right]_t = \left[VOC_i\right]_0 \times exp\left(-k_{OHi}[\cdot\mathrm{OH}]\Delta t\right) \quad (1)$$

$$[\cdot OH]\Delta t = \frac{1}{(k_E - k_X)[OH]} \times \left[In\left(\frac{E}{X}t = 0\right) - In\left(\frac{E}{X}t = t\right)\right] \quad (2)$$

Where $[VOC_i]_t$ and $[VOC_i]_0$ represent the measured value and initial concentration of VOC_i, respectively. K_E and K_X are the OH reaction rate constants for ethylbenzene and m,p-xylene, respectively. $(E/X)_{t=0}$ is the initial concentration ratio of ethylbenzene to m,p-xylene during the time of fresh emissions. $(E/X)_{t=t}$ is the concentration ratio of ethylbenzene to m,p-xylene at time t. Only eight online monitoring sites (LND_UB, MAR_UB, PAR_UB, STB_UB, ZUR_UB, LND_TR, LYO1_IND, LYO2_IND) with hourly resolution EX data were monitored.

The hourly variations of the E/X ratios throughout the year and across different seasons for each site are shown in Fig. S28. The measured E/X ratios remained relatively stable and low from 00:00 to 05:00 LT. This time range represents the minimum E/X ratio and is assumed to indicate fresh emissions, likely without photochemical losses. In this study, we selected the median E/X ratio from 00:00 to 05:00 LT across all sites, which is 0.35, as $(E/X)_{t=0}$. The initial concentrations of VOC species were then estimated for all sites over time. However, due to the fact that some sites measure VOCs with a resolution of 1 day or 2 days, there are certain inaccuracies in the initial concentrations.

Maximum O_3 formation potential (MOFP) and SOA formation potential (SOAP) of VOCs

For a group of 20 widely measured VOCs (n-butane, n-pentane, i-pentane, n-hexane, n-heptane, n-octane, i-octane, 1,3-butadiene, 1-butene, trans-2-butene, cis-2-butene,1-pentene, benzene, toluene, ethylbenzene, m,p-xylene, o-xylene,1,2,4-trimethylebenzene, 1,3,5-trimethylebenzene, and isoprene), the Maximum O_3 Formation Potential (MOFP) and SOA Formation Potential (SOAP) were used to evaluate the contribution of VOC species to O_3 and SOA formation, respectively. The MOFP and SOAP values were calculated using the following equations:

$$MPFP_i = \left[VOC_i\right] \times MIR_i \quad (3)$$

where $[VOC_i]$ represents the mixing ratio of VOC species i, and MIR_i is the maximum incremental reactivity, which quantifies the mass of O_3 produced per unit mass of VOC species added[62,63]

$$SOAP_i = \left[VOC_i\right] \times Y_{SOAi} \quad (4)$$

where $SOAP_i$ is calculated by multiplying the ambient initial concentration $[VOC_i]$ with the SOA yield $Y_{SOA,i}$. The SOA yields were derived from Gu et al.[11], based on smog chamber experiments and the two-product model for a comprehensive inventory of VOCs.

Subsequently, the VOC species were ranked from highest to lowest based on their percentile contributions to the MOFP and SOAP. It is important to note that this analysis relies on several key assumptions to simplify the complex nature of atmospheric chemistry: (1) the contribution of each VOC species to O_3 and SOA formation was evaluated independently, without accounting for potential synergistic or antagonistic interactions among species; (2) the SOA yields were derived from controlled laboratory experiments, which may not fully capture the variability and complexity of real-world atmospheric conditions; and (3) the calculations assumed uniform environmental influences, such as temperature, photochemical activity, and background NO_X levels, across all monitoring sites. While these assumptions enable a consistent and comparable analysis, they also represent inherent limitations. Future studies employing more advanced modeling approaches and real-world data are recommended to address these complexities.

Physiologically based toxicokinetic (PBTK) modeling

PBTK modeling was implemented using the *R* package *httk*, developed and maintained by the U.S. EPA[36], which provides a high-throughput platform for simulating human toxicokinetics. This package integrates previously validated PBTK structures[64] and physicochemical parameters derived from the EPA CompTox Chemicals Dashboard, allowing consistent and reproducible modeling of ADME. In this study, four representative VOCs

(benzene, toluene, ethylbenzene, and 1,2,4-trimethylbenzene) were selected based on their prevalence in urban environments and the availability of validated toxicokinetic parameters within the *httk* database. Simulations were conducted using the gas-phase inhalation PBTK model implemented in *httk* (solve_gas_pbtk), which allows ambient air concentrations to be directly specified as inhalation exposure inputs. Ambient VOC concentrations measured at monitoring sites were converted from parts per trillion by volume (ppt) to parts per million by volume (ppm) and used as the exposure concentration parameter (exp.conc). The daily inhalation exposure duration was set to 8 h (exp.duration = 8), representing typical outdoor exposure conditions. Chemical-specific parameters were obtained by specifying the CAS numbers of the target compounds within *httk* (e.g., 1,2,4-trimethylbenzene, CAS No. 95-63-6). Physiological parameters (e.g., body weight, organ volumes, blood flows, and ventilation rate) were set to the default human configuration in *httk*, corresponding to a reference adult (70 kg). Because the maximal metabolic rate parameter (Vmax) was set to zero in the default configuration, hepatic metabolism was modeled as first-order clearance. Detailed chemical and physiological parameters are provided in Supplementary Tables S4 and S5.

It is assumed that all physiological compartments (organs/tissues) are governed by the concentrations of chemicals entering the body. The human body was represented by seven interconnected physiological compartments, including the lung, gut, liver, kidney, arterial blood, venous blood, and the rest of the body. The "rest" compartment aggregates all organs/tissues not explicitly modeled (e.g., adipose, brain, skin, heart, bone marrow, and muscle)[36]. Its organ–plasma partition coefficient is calculated as the volume-weighted average of the remaining organs' coefficients, thereby accounting for their relative physiological contributions to systemic distribution. The model assumes perfusion-limited distribution, where each organ rapidly reaches equilibrium with the circulating blood. Metabolism is restricted to the liver, which is considered the sole metabolic organ, while the kidneys represent the exclusive route of excretion. The compartments are interconnected through arterial and venous blood flows, simulating chemical transfer and clearance across the systemic circulation. The general structure of the model is shown in Fig. S29.

To represent continuity in exposure over time, we implemented a rolling exposure framework inspired by Hua et al.[65] for the four VOCs. In this framework, internal concentrations at each time step are determined by both newly inhaled chemicals during the daily outdoor exposure period (8 h) and the residual fraction remaining after physiological processing from the previous day. Although for the four VOCs under typical ambient exposures rapid metabolism and elimination imply that carry-over concentrations from the previous day are generally minimal, the rolling framework preserves the continuous nature of toxicokinetic processes rather than treating daily exposures as independent events. Model outputs were summarized as the maximum internal concentrations achieved within each daily exposure period (daily peak concentrations) for each organ and compartment. These daily peak values were used to characterize organ-specific internal exposure patterns across sites and compounds. Differences in modeled internal VOC concentrations among organs and across sites were evaluated using the Kruskal–Wallis test due to non-normal data distributions.

Data availability

Data availability: All data supporting the findings of this study are included in the Article and its Supplementary Information. Additional processed datasets generated during the current study are available from the corresponding author upon reasonable request.

Code availability

The analysis in this study was performed using R package version 6.5-0 and the *httk* package for physiologically based toxicokinetic modeling. Custom scripts used for data processing, statistical analysis, and figure generation are available from the corresponding author upon reasonable request.

Received: 18 December 2025; Accepted: 3 March 2026;
Published online: 20 March 2026

References

1. Yue, X. et al. Mitigation of indoor air pollution: a review of recent advances in adsorption materials and catalytic oxidation. *J. Hazard. Mater.* **405**, 124138 (2021).
2. Duan, C., Liao, H., Wang, K. & Ren, Y. The research hotspots and trends of volatile organic compound emissions from anthropogenic and natural sources: a systematic quantitative review. *Environ. Res.* **216**, 114386 (2023).
3. Haagen-Smit, A. J. Chemistry and physiology of Los Angeles smog. *Ind. Eng. Chem.* **44**, 1342–1346 (1952).
4. Grosjean, D. & Seinfeld, J. H. Parameterization of the formation potential of secondary organic aerosols. *Atmos. Environ. (1967)* **23**, 1733–1747 (1989).
5. Derwent, R. G. et al. Secondary organic aerosol formation from a large number of reactive man-made organic compounds. *Sci. Total Environ.* **408**, 3374–3381 (2010).
6. Meng, Y. et al. Ambient volatile organic compounds at a receptor site in the Pearl River Delta region: variations, source apportionment and effects on ozone formation. *J. Environ. Sci.* **111**, 104–117 (2022).
7. Pandey, P. & Yadav, R. A review on volatile organic compounds (VOCs) as environmental pollutants: fate and distribution. *Int. J. Plant Env.* **4**, 14–26 (2018).
8. Zhou, X., Zhou, X., Wang, C. & Zhou, H. Environmental and human health impacts of volatile organic compounds: a perspective review. *Chemosphere* **313**, 137489 (2023).
9. Guo, H. et al. Tropospheric volatile organic compounds in China. *Sci. Total Environ.* **574**, 1021–1043 (2017).
10. Baudic, A. et al. Seasonal variability and source apportionment of volatile organic compounds (VOCs) in the Paris megacity (France). *Atmos. Chem. Phys.* **16**, 11961–11989 (2016).
11. Gu, S., Guenther, A. & Faiola, C. Effects of anthropogenic and biogenic volatile organic compounds on Los Angeles air quality. *Environ. Sci. Technol.* **55**, 12191–12201 (2021).
12. Cui, L. et al. Measurement report: ambient volatile organic compound (VOC) pollution in urban Beijing: characteristics, sources, and implications for pollution control. *Atmos. Chem. Phys.* **22**, 11931–11944 (2022).
13. Mcdonald, B. C. et al. Volatile chemical products emerging as largest petrochemical source of urban organic emissions. *Science* **359**, 760–764 (2018).
14. Aqeg-Eu, Non-methane Volatile Organic Compounds in the UK. Department for Environment, Food and Rural Affairs; Scottish Government; Welsh Government; and Department of Agriculture, Environment and Rural Affairs in Northern Ireland. https://uk-air.defra.gov.uk (2020).
15. Emep-Ceip, EMEP Centre on Emission Inventories and Projections. Official Emission Inventories, Data Viewer. https://www.ceip.at/data-viewer-2/overview-dataviewers.
16. EC, Proposal for a Directive of the European Parliament and of the Council on ambient air quality and cleaner air for Europe (recast). Europa Consilium and European Parliament. Agreement of 8th March 2024. https://data.consilium.europa.eu/doc/document/ST-7335-2024-INIT/en/pdf.
17. Lin, N. et al. Estimation of dermal exposure to volatile organic compounds (VOCs) from feminine hygiene products: integrating measurement data and physiologically based toxicokinetic (PBTK) model. *Environ. Health Perspect.* **133**, 067020 (2025).
18. Ding, N., Lin, N., Batterman, S. & Park, S. K. Feminine hygiene products and volatile organic compounds in reproductive-aged women across the menstrual cycle: a longitudinal pilot study. *J. Women's. Health* **31**, 210–218 (2022).

19. Hu, M. et al. Physiologically-based toxicokinetic modeling of human dermal exposure to diethyl phthalate: application to health risk assessment. *Chemosphere* **307**, 135931 (2022).
20. Xie, R. et al. In vitro to in vivo extrapolation for predicting human equivalent dose of phenolic endocrine disrupting chemicals: PBTK model development, biological pathways, outcomes and performance. *Sci. Total Environ.* **897**, 165271 (2023).
21. Georgopoulos, P. G. et al. Reconstructing population exposures to environmental chemicals from biomarkers: challenges and opportunities. *J. Expo. Sci. Environ. Epidemiol.* **19**, 149–171 (2009).
22. Kim, D. et al. PBTK modeling demonstrates contribution of dermal and inhalation exposure components to end-exhaled breath concentrations of naphthalene. *Environ. Health Perspect.* **115**, 894–901 (2007).
23. Hellén, H., Tykkä, T. & Hakola, H. Importance of monoterpenes and isoprene in urban air in northern Europe. *Atmos. Environ. (1994)* **59**, 59–66 (2012).
24. Gu, Y. et al. Source apportionment of consumed volatile organic compounds in the atmosphere. *J. Hazard. Mater.* **459**, 132138 (2023).
25. Liu, B. et al. Effect of photochemical losses of ambient volatile organic compounds on their source apportionment. *Environ. Int.* **172**, 107766 (2023).
26. In'T Veld, M. et al. Identification of volatile organic compounds and their sources driving ozone and secondary organic aerosol formation in NE Spain. *Sci. Total Environ.* **906**, 167159 (2024).
27. Brito, J. et al. Vehicular emission ratios of VOCs in a megacity impacted by extensive ethanol use: results of ambient measurements in Sao Paulo, Brazil. *Environ. Sci. Technol.* **49**, 11381–11387 (2015).
28. Cao, M., Chen, M., Ge, P., Cui, Y. & Li, W. Seasonal variation, source contribution, and impact factors of biogenic organic aerosols in PM2. 5 in Nanjing, China. *Sci. Total Environ.* **843**, 156875 (2022).
29. Waked, A. et al. Multi-year levels and trends of non-methane hydrocarbon concentrations observed in ambient air in France. *Atmos. Environ. (1994)* **141**, 263–275 (2016).
30. Dufresne, M. et al. Volatile organic compound sources and impacts in an urban Mediterranean area (Marseille, France). *Atmos. Chem. Phys.* **25**, 5977–5999 (2025).
31. Gu, C. et al. Investigation on the urban ambient isoprene and its oxidation processes. *Atmos. Environ. (1994)* **270**, 118870 (2022).
32. Wang, H., Liu, X., Wu, C. & Lin, G. Regional to global distributions, trends, and drivers of biogenic volatile organic compound emission from 2001 to 2020. *Atmos. Chem. Phys.* **24**, 3309–3328 (2024).
33. Stavrakou, T. et al. Isoprene emissions over Asia 1979–2012: impact of climate and land-use changes. *Atmos. Chem. Phys.* **14**, 4587–4605 (2014).
34. Mcgenity, T. J., Crombie, A. T. & Murrell, J. C. Microbial cycling of isoprene, the most abundantly produced biological volatile organic compound on Earth. *ISME J.* **12**, 931–941 (2018).
35. Bolden, A. L., Kwiatkowski, C. F. & Colborn, T. New look at BTEX: are ambient levels a problem? *Environ. Sci. Technol.* **49**, 5261–5276 (2015).
36. Pearce, R. et al. httk: High-Throughput Toxicokinetics. *J. Stat. Softw*. **79**, 1-26 (2025).
37. Kim, S. et al. Toluene concentrations in the blood and risk of thyroid cancer among residents living near national industrial complexes in South Korea: a population-based cohort study. *Environ. Int.* **146**, 106304 (2021).
38. Caporale, N. et al. From cohorts to molecules: adverse impacts of endocrine disrupting mixtures. *Science* **375**, e8244 (2022).
39. Liew, Z. & Guo, P. Human health effects of chemical mixtures. *Science* **375**, 720–721 (2022).
40. Le Bras, Z., Rubli, P., Hueglin, C. & Reimann, S. Measurement report: 30 years of BTEX monitoring at a suburban site in Switzerland supported by additional urban VOC observations. *Atmos. Chem. Phys.* **26**, 869–878 (2026).
41. Tinel, L. et al. *Determining Volatile Organic Compounds (VOC) and Particulate Matter (PM1) Shipping Emission Factors from Land-based, High Time Resolution Observations in an Emission Control Area of Northern France*. (Copernicus Meetings, 2025).
42. Vestreng, V. et al. Evolution of NOx emissions in Europe with focus on road transport control measures. *Atmos. Chem. Phys.* **9**, 1503–1520 (2009).
43. Heeb, N. V. et al. A comparison of benzene, toluene and C2-benzenes mixing ratios in automotive exhaust and in the suburban atmosphere during the introduction of catalytic converter technology to the Swiss Car Fleet. *Atmos. Environ.* **34**, 3103–3116 (2000).
44. Laurent, A. & Hauschild, M. Z. Impacts of NMVOC emissions on human health in European countries for 2000–2010: use of sector-specific substance profiles. *Atmos. Environ.* **85**, 247–255 (2014).
45. Ec, COMMISSION REGULATION (EU) 2017/1151 of 1 June 2017 supplementing Regulation (EC) No 715/2007 of the European Parliament and of the Council on type-approval of motor vehicles with respect to emissions from light passenger and commercial vehicles (Euro 5 and Euro 6) and on access to vehicle repair and maintenance information, amending Directive 2007/46/EC of the European Parliament and of the Council, Commission Regulation (EC) No 692/2008 and Commission Regulation (EU) No 1230/2012 and repealing Commission Regulation (EC) No 692/2008. (2017).
46. Jhang, S., Fang, G., Cheng, W. L., Lee, K. & Lin, Y. Impact of ethanol-gasoline implementation on regulated and unregulated emissions from Euro 3–5 standard vehicles over the WLTP driving cycle. *Environ. Monit. Assess.* **197**, 954 (2025).
47. Eu, DIRECTIVE (EU) 2016/2284 OF THE EUROPEAN PARLIAMENT AND OF THE COUNCIL of 14 December 2016 on the reduction of national emissions of certain atmospheric pollutants, amending Directive 2003/35/EC and repealing Directive 2001/81/EC. (2016).
48. Sebos, I. & Kallinikos, L. E. Modelling of NMVOC emissions from solvents use in Greece. *IOP Conf. Ser. Earth Environ. Sci.* **1123**, 12072 (2022).
49. Shaw, A. A., Steketee, J. D., Bukiya, A. N. & Dopico, A. M. Toluene toxicity in the brain: from cellular targets to molecular mechanisms. *Annu. Rev. Pharmacol. Toxicol.* **65**, 487–506 (2025).
50. Abubakar, M. G., Hamza, A. B., Ibrahim, A. G. & Rabiu, S. Toxicological impact of petroleum vapours on liver and kidney function: a comprehensive review. *Direct Res. J. Public Health Environ. Technol.* **10**, 31–57 (2025).
51. Xie, Y., Peng, R. & Xiao, L. Environmental chemicals and female reproductive health: unraveling mechanisms and societal impacts—a narrative review. *Clin. Exp. Obstet. Gynecol.* **52**, 39882 (2025).
52. Simon, L. L. et al. Two years of volatile organic compound online in situ measurements at the Site Instrumental de Recherche par Télédétection Atmosphérique (Paris region, France) using proton-transfer-reaction mass spectrometry. *Earth Syst. Sci. Data* **15**, 1947–1968 (2023).
53. Laj, P. et al. Aerosol, clouds and trace gases research infrastructure-ACTRIS, the European research infrastructure supporting atmospheric science. *Bull. Am. Meteorol. Soc.* **105**, 1098–1136 (2024).
54. Schwartz, S. E. & Warneck, P. Units for use in atmospheric chemistry (IUPAC Recommendations 1995). *Pure Appl. Chem.* **67**, 1377–1406 (1995).
55. Kruskal, W. H. & Wallis, W. A. Use of ranks in one-criterion variance analysis. *J. Am. Stat. Assoc.* **47**, 583–621 (1952).
56. Mann, H. B. Nonparametric tests against trend. *Econ.* **13**, 245–259 (1945).
57. Kendall, M. G., Gibbons, J. D. *Rank Correlation Methods*. (Oxford University Press, 1990).
58. Salmi, T. *Detecting Trends of Annual Values of Atmospheric Pollutants by the Mann-Kendall Test and Sen's Slope Estimates—The Excel Template Application MAKESENS* (Ilmatieteen laitos, 2002).

59. Muggeo, V. M. Segmented: an R package to fit regression models with broken-line relationships. *R. N.* **8**, 20–25 (2008).
60. Balduzzi, S., Rücker, G. & Schwarzer, G. How to perform a meta-analysis with R: a practical tutorial. *BMJ Ment. Health* **22**, 153–160 (2019).
61. Mckeen, S. A. & Liu, S. C. Hydrocarbon ratios and photochemical history of air masses. *Geophys. Res. Lett.* **20**, 2363–2366 (1993).
62. Carter, W. P. Development of the SAPRC-07 chemical mechanism. *Atmos. Environ.* **44**, 5324–5335 (2010).
63. Venecek, M. A., Carter, W. P. & Kleeman, M. J. Updating the SAPRC maximum incremental reactivity (MIR) scale for the United States from 1988 to 2010. *J. Air Waste Manage. Assoc*. **68**, 1301–1316 (2018).
64. Jongeneelen, F. J. & Berge, W. F. T. A generic, cross-chemical predictive PBTK model with multiple entry routes running as application in MS Excel; design of the model and comparison of predictions with experimental results. *Ann. Occup. Hyg.* **55**, 841–864 (2011).
65. Hua, C. et al. Internal exposure risks of particle-bound polycyclic aromatic hydrocarbons with an hourly time resolution to humans in Beijing. *Environ. Sci. Technol*. **59**, 12035-12047 (2025).

Acknowledgements

This study is supported by the RI-URBANS project (Research Infrastructures Services Reinforcing Air Quality Monitoring Capacities in European Urban & Industrial Areas, European Union's Horizon 2020 research and innovation program, Green Deal, European Commission, contract 101036245). This project was also supported by Guangdong Basic and Applied Basic Research Foundation (2026A1515030034), part funded by the National Natural Science Foundation of China (42407566, 42205099), and Introduction Innovative and Research Teams Project of Guangdong Pearl River Talents Program (2023ZT10L102). VOC data was assessed and evaluated by two ACTRIS CiGas (https://www.actris.eu/topical-centre/cigas) units at IMT Nord Europe - France and EMPA - Switzerland based on ACTRIS recommendations and guidelines. AMYS acknowledges the "Agencia Estatal de Investigación" from the Spanish Ministry of Science, Innovation and Universityes for her Ramon y Cajal grant (RYC2021-032519-I) and the support from the Consolidación Investigadora project (CNS2022-135757). RS acknowledges a Ramón y Cajal grant (RYC2020-029216-I) funded by MCIN/AEI/ 10.13039/501100011033 and by "ESF Investing in your future". IDAEA-CSIC is a Severo Ochoa Center of Research Excellence (MCIN/AEI, Project CEX2018-000794-S). Observations at the BAQS-UB in the United Kingdom was supported by Natural Environment Research Council (NE/T001976/1) and the Department for Environment, Food and Rural Affairs.

Author contributions

Xiansheng Liu: Writing-original draft, Writing-review & editing, Conceptualization. Minghan Wang, Taicheng An, Xun Zhang, Tao Wang, Rosa Lara: Methodology. Marta Monge: Project administration. Marvin Dufresne, Ana Maria Yañez-Serrano, Roger Seco, Marie Gohy, Paul Petit, Audrey Chevalier, Marie-Pierre Vagnot, Yann Fortier, Alexia Baudic, Véronique Ghersi, Grégory Gille, Ludovic Lanzi, Valérie Gros, Jean-Eudes Petit, Heidi Hellén, Leïla Simon, Stefan Reimann, Zoé Le Bras, Michelle Jessy Müller, David Beddows, Siqi Hou, Zongbo Shi, Roy M Harrison, William Bloss, James Dernie, Stéphane Sauvage, Alastair Lewis, Jim Hopkins: Data curation. Xiaoli Duan, Philip K. Hopke, Andrés Alastuey, Thérèse Salameh: Writing—review & editing. Xavier Querol: Writing—review & editing, supervision, project administration, funding acquisition, data curation, conceptualization.

Competing interests

Author Xavier Querol is a member of the Editorial Board of npj Climate and Atmospheric Science. He was not involved in the journal's review of, or decisions related to, this manuscript. The remaining authors declare no competing interests.

Additional information

Supplementary information The online version contains supplementary material available at https://doi.org/10.1038/s41612-026-01378-9.

Correspondence and requests for materials should be addressed to Xiansheng Liu, Xun Zhang or Thérèse Salameh.

[1]Guangdong Key Laboratory of Environmental Catalysis and Health Risk Control, Guangdong-Hong Kong-Macao Joint Laboratory for Contaminants Exposure and Health, Institute of Environmental Health and Pollution Control, Guangdong University of Technology, Guangzhou 510006, China. [2]Guangzhou Key Laboratory of Environmental Catalysis and Pollution Control, Guangdong Technology Research Center for Photocatalytic Technology Integration and Equipment Engineering, School of Environmental Science and Engineering, Guangdong University of Technology, Guangzhou 510006, China. [3]Beijing Key Laboratory of Big Data Technology for Food Safety, School of Computer and Artificial Intelligence, Beijing Technology and Business University, Beijing 100048, China. [4]Shanghai Key Laboratory of Atmospheric Particle Pollution and Prevention, Department of Environmental Science & Engineering, Fudan University, Shanghai 200433, China. [5]Institute of Environmental Assessment and Water Research (IDAEA-CSIC), 08034 Barcelona, Spain. [6]IMT Nord Europe, Institut Mines-Télécom, University of Lille, Centre for Energy and Environment, F-59000 Lille, France. [7]CREAF, E08193 Bellaterra (Cerdanyola del Vallès), Catalonia, Barcelona, Spain. [8]CSIC, Global Ecology Unit, CREAF-CSIC-UAB, E08193 Bellaterra (Cerdanyola del Vallès), Catalonia, Barcelona, Spain. [9]Institut Scientifique de Service Public (ISSeP), 4000 Liège, Belgium. [10]Atmo Grand-Est (AtmoGE), 67300 Schiltigheim, France. [11]Atmo Auvergne-Rhône-Alpes (AtmoAURA), 69500 Bron, France. [12]Airparif, Air Quality Monitoring Network for the Greater Paris area, 7 rue Crillon, 75004 Paris, France. [13]AtmoSud, 13006 Marseille, France. [14]Laboratoire des Sciences du Climat et de l'Environnement (CEA-CNRS-UVSQ, IPSL), CAE/Orme des Merisiers, 91191 Gif sur Yvette, France. [15]PSI Center for Energy and Environmental Sciences, 5232 Villigen PSI, Switzerland. [16]Finish Meteorological Institute (FMI), FI-00560 Helsinki, Finland. [17]Swiss Federal Laboratories for Materials Science and Technology (Empa), 8600 Dübendorf, Switzerland. [18]School of

Geography Earth and Environmental Sciences, University of Birmingham, B15 2TT Birmingham, United Kingdom. [19]Ricardo, W2 6LA, London, United Kingdom. [20]Wolfson Atmospheric Chemistry Laboratories, Department of Chemistry, University of York, Heslington, York YO10 5DD, UK. [21]School of Energy and Environmental Engineering, University of Science and Technology Beijing, Beijing, China. [22]Institute for a Sustainable Environment, Clarkson University, Potsdam, NY 13699, USA. [23]Department of Public Health Sciences, University of Rochester School of Medicine and Dentistry, Rochester, NY 14642, USA.
✉e-mail: xianshengliu@gdut.edu.cn; zhangxun@btbu.edu.cn; therese.salameh@imt-nord-europe.fr